# Investigation of three-pulse photon echo in thick crystal using finite-difference time-domain method*

Xiu-Rong Ma(马秀荣)[1], Lin Xu(徐林)[2,†], Shi-Yuan Chang(常世元)[3], and Shuang-Gen Zhang(张双根)[4]

[1] Department of Computer and Communication Engineering, Tianjin University of Technology, Tianjin 300384, China
[2] Engineering Research Center of Communication Devices and Technology, Ministry of Education, Tianjin Key Laboratory of Film Electronic and Communication Devices, Tianjin 300384, China

(Received 20 October 2016; revised manuscript received 1 December 2016; published online 10 March 2017)

This paper investigates the phenomenon of three-pulse photon echo in thick rare-earth ions doped crystal whose thickness is far larger than 0.002 cm which is adopted in previous works. The influence of thickness on the three-pulse photon echo's amplitude and efficiency is analyzed with the Maxwell–Bloch equations solved by finite-difference time-domain method. We demonstrate that the amplitude of three-pulse echo will increase with the increasing of thickness and the optimum thickness to generate three-pulse photon echo is 0.3 cm for $Tm^{3+}$:YAG when the attenuation of the input pulse is taken into account. Meanwhile, we find the expression $0.09\exp(\alpha' L)$, which is previously employed to describe the relationship between echo's efficiency and thickness, should be modified as $1.3\cdot 0.09\exp(2.4\cdot\alpha' L)$ with the propagation of echo considered.

**Keywords:** three-pulse photon echo, Maxwell–Bloch equations, finite-difference time-domain method

**PACS:** 42.50.Md, 03.65.Sq, 14.70.Bh **DOI:** 10.1088/1674-1056/26/4/044201

## 1. Introduction

The three-pulse photon echo (3PE) is derived from the interaction between a sequence of optical pulses and an inhomogeneously broadened crystal. This phenomenon is widely applied in optical information storage[1–3] and arbitrary waveform generation.[4–6] In previous papers, the convolution product of the input pulses' electric field {Eq. (6) of Ref. [3]} or the product of propagators {Eq. (1) of Ref. [7]} are used to describe the 3PE. Our group had directly deduced the analytical solution of the 3PE based on Bloch equations.[8] The methods mentioned above have a flaw in common: the effect of propagation is not taken into consideration and the influence of crystal's thickness on 3PE is ignored. This drawback can be compensated by Maxwell–Bloch (M-B) equations. However, the M-B equations are difficult to be solved directly due to the integral for coupling variables.

The difficulty mentioned above can be overcome by means of finite-difference time-domain (FDTD) method proposed by Ziolkowski *et al.* in 1995.[9] They transform the M-B equations into discrete version to get the numerical solutions for each variable with iteration. This excellent method has been used to investigate the phenomenon of 3PE.[10,11] However, the thickness of the crystal in their simulation is only set as 0.002 cm which is smaller than the actual situation.

In this paper, we investigate the phenomenon of three-pulse photon echo in thick rare-earth ions doped crystal such as $Tm^{3+}$:YAG, where the effect of thickness should be taken into consideration. Firstly, the propagation equation is deduced based on M-B equations. With the numerical solutions of M-B equations obtained by FDTD methods, the interaction between one pulse and crystal is presented. Then, this method is utilized to explore the formation of 3PE in which the influence of input pulses' area is analyzed. At last, the influence of thickness on 3PE's amplitude and efficiency is investigated. According to the simulation results, we find that the amplitude of the 3PE will increase with the increasing of crystal's thickness and the optimum thickness to generate 3PE is 0.3 cm for $Tm^{3+}$:YAG when the attenuation of the input pulse is considered. Meanwhile, the variation of 3PE's efficiency is presented and the expression used to describe the relationship between echo's efficiency and thickness is proposed.

## 2. Basic principle

### 2.1. Influence of input pulse on polarization

During the interaction between the optical pulse and the crystal, the input field acts as a source to drive the polarization of the medium. For a quasi-monochromatic field, the polarization induced in the medium is also quasi-monochromatic which is expressed as $\boldsymbol{P}(z,t) = P(z,t)\,\mathrm{e}^{\mathrm{i}[kz-\omega_0 t]}$. $P(z,t)$ is the complex amplitude of the polarization, $k = \omega_0/c$ is the wave number, $\omega_0$ is the central frequency of the optical pulse, $c$ is the speed of light in the crystal.

The $P(z,t)$ mentioned above is associated with the microcosmic dipole moment $\rho_{\mathrm{ab}}(z,t)$[12]

$$P(z,t) = N_{\mathrm{atom}}\wp\rho_{\mathrm{ab}}(z,t)$$

*Project supported by Tianjin Research Program Application Foundation and Advanced Technology, China (Grant No. 15JCQNJC01100).
†Corresponding author. E-mail: xulin_tjut@139.com
© 2017 Chinese Physical Society and IOP Publishing Ltd 

$$= \frac{1}{2} N_{\text{atom}} \wp [u(z,t) - iv(z,t)], \tag{1}$$

where $N_{\text{atom}}$ is the total number of atoms, $\wp$ is the dipole matrix element of the transition. $u(z,t)$ is the real part of $\rho_{\text{ab}}(z,t)$ which represents dispersion; $v(z,t)$ is the imaginary part of $\rho_{\text{ab}}(z,t)$ which represents absorption. They are derived from Bloch equations.

The Bloch equations in rotating frame can be written as

$$\dot{u}(z,t) = -\Delta \cdot v(z,t) - \frac{u(z,t)}{T_2}, \tag{2a}$$

$$\dot{v}(z,t) = \Delta \cdot u(z,t) + \frac{\wp \varepsilon(z,t)}{\hbar} \cdot w(z,t) - \frac{1}{T_2} \cdot v(z,t), \tag{2b}$$

$$\dot{w}(z,t) = -\frac{\wp \varepsilon(z,t)}{\hbar} \cdot v(z,t) - \frac{w(z,t)+1}{T_1}, \tag{2c}$$

where $w(z,t)$ represents the population inversion. $u(z,t)$, $v(z,t)$, and $w(z,t)$ constitute the Bloch vector $\boldsymbol{B} = [u(z,t), v(z,t), w(z,t)]$. $\Delta = \omega_{\text{ab}} - \omega_0$ denotes the detuning of $\omega_0$ from the atom's resonant frequency $\omega_{\text{ab}}$. $\varepsilon(z,t)$ is the envelope of the incident field. To realize the sudden removing of the input pulse, the stark effect[13] is utilized. Under this circumstance, $\Delta$ will change into $\Delta' = \omega_{\text{ab}} + \delta\omega - \omega_0$ where $\delta\omega$ is the frequency shift of atoms caused by stark effect. $\hbar$ is Planck constant. $T_2$ and $T_1$ are the coherence time and the population lifetime of the crystal, respectively. For $Tm^{3+}$:YAG, $T_2 \approx 10$ μs and $T_1 \approx 10$ ms.

Equations (1) and (2) show that the input pulse will alter the values of dispersion $u(z,t)$ and absorption $v(z,t)$ which lead to the change of polarization.

### 2.2. Deduction of propagation equation

The crystal's polarization induced by the incident pulse will influence the field during the propagation which is expressed by Maxwell equations

$$-\nabla^2 \boldsymbol{E}(z,t) + \frac{1}{c^2} \frac{\partial^2 \boldsymbol{E}(z,t)}{\partial t^2} = -\mu \frac{\partial^2 \boldsymbol{P}(z,t)}{\partial t^2}, \tag{3}$$

where $\boldsymbol{E}(z,t) = \varepsilon(z,t)\, e^{i[kz-\omega_0 t]}$, $\mu$ is the permeability of crystal.

With slowly-varying envelope approximation,[14] equation (3) can be rewritten as

$$\frac{\partial \varepsilon(z,t)}{\partial z} + \frac{1}{c} \frac{\partial \varepsilon(z,t)}{\partial t} = -\frac{k}{2\varepsilon} \text{Im}[P(z,t)], \tag{4}$$

where $\varepsilon$ is the permeability of crystal.

Casting Eq. (1) into Eq. (6), we can obtain

$$\frac{\partial \varepsilon(z,t)}{\partial z} + \frac{1}{c} \frac{\partial \varepsilon(z,t)}{\partial t} = \frac{k}{4\varepsilon} N_{\text{atom}} \wp v(z,t). \tag{5}$$

In this paper, the steady-state limit is taken into consideration which is expressed as[14]

$$\frac{\partial \varepsilon(z,t)}{\partial t} = 0. \tag{6}$$

Combing the Eqs. (5) and (6), the total differential equation of the electric field can be described as

$$\begin{aligned} &\varepsilon(z+\mathrm{d}z, t+\mathrm{d}t) - \varepsilon(z,t) \\ &= \frac{\partial \varepsilon(z,t)}{\partial z} \mathrm{d}z + \frac{\partial \varepsilon(z,t)}{\partial t} \mathrm{d}t \\ &= \frac{k}{4\varepsilon} N_{\text{atom}} \wp v(z,t)\, \mathrm{d}z \\ &= \frac{\alpha' n \hbar}{4\pi \wp g(0)} v(z,t)\, \mathrm{d}z, \end{aligned} \tag{7}$$

where $\varepsilon(z+\mathrm{d}z, t+\mathrm{d}t)$ is the new envelop after the optical pulse propagates $\mathrm{d}z$ distance, $\alpha'$ is linear resonant absorption coefficient,[15] $n$ is the index of refraction, $g(0) = 1/\sqrt{\pi}\delta_{\text{in}}$, $\delta_{\text{in}}$ is the inhomogeneous width of the crystal.

Equation (7) is the propagation equation which establishes a relationship between the absorption $v(z,t)$ and the $\varepsilon(z+\mathrm{d}z, t+\mathrm{d}t)$.

### 2.3. Interaction between one pulse and the crystal

Equations (2) and (7) describe the interaction between optical pulses and the crystal. Here, we investigate the interaction between one pulse and the crystal. According to the experiment results,[16,17] we depict the schematic diagram of this interaction in Fig. 1.

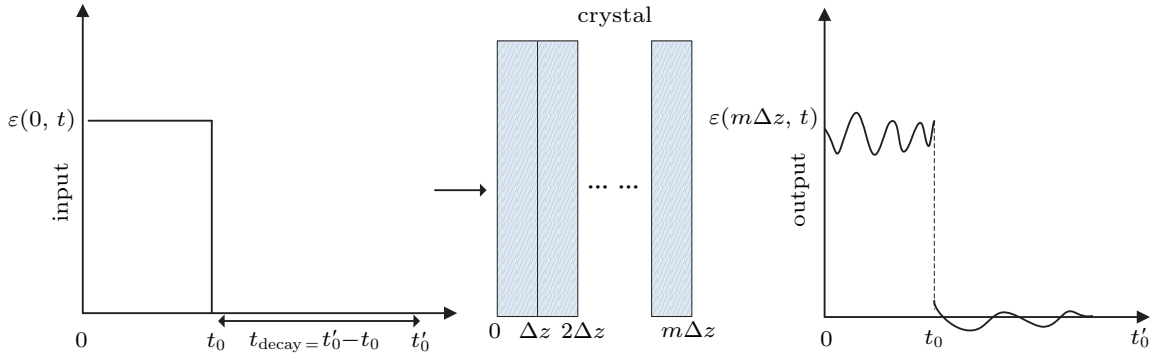



**Fig. 1.** (color online) Schematic diagram of the interaction between one optical pulse and the crystal.

As is seen in Fig. 1, the output of the incident pulse will be in fluctuation and the induced field will not turn to 0 immediately when the incident pulse vanished.

We simulate this interaction with FDTD method. This method transforms $z$ and $t$ into discrete version $\Delta z$ and $\Delta t$. The value of $\Delta z$ should not exceed $\lambda/100$, where $\lambda$ is the wavelength. The value of $\Delta t$ is less than $\Delta z/c$.[9] In this paper, we set $\lambda = 793\times10^{-9}$ m, $\Delta z = \lambda/200$, and $\Delta t = \Delta z/2c$.

At first, we initialize the basic parameters. For $Tm^{3+}$:YAG, $n = 1.4612$ and $\delta_{\text{in}} = 30$ GHz. $\alpha'$ is equal to 280 when the $N_{\text{atom}}$ is set as $4.61\times10^{23}$ m$^{-3}$. The Bloch vectors are set as $\boldsymbol{B} = [0,0,-1]$ which means that the crystal is in absorbing state at the beginning. The $\Delta$ is set as 0 which means that the interaction is strictly resonate. The duration of input pulse is set as $5\times10^{-9}$ s and the area of the pulse $\theta = (\wp/\hbar)\int\mathcal{E}(0,t)\,\mathrm{d}t$ is set as $\pi/2$. The d$t$ is set as $n'\Delta t = 1\times10^{-11}$ s, where$n' = 1513200$. The $t_{\text{decay}}$ is set as $1000n'\Delta t = 10\times10^{-9}$ s which is far less than $T_1$ and $T_2$. The thickness of crystal is set as $L = 0.01$ cm. Figure 2 shows the simulation results of the interaction between one pulse and crystal.

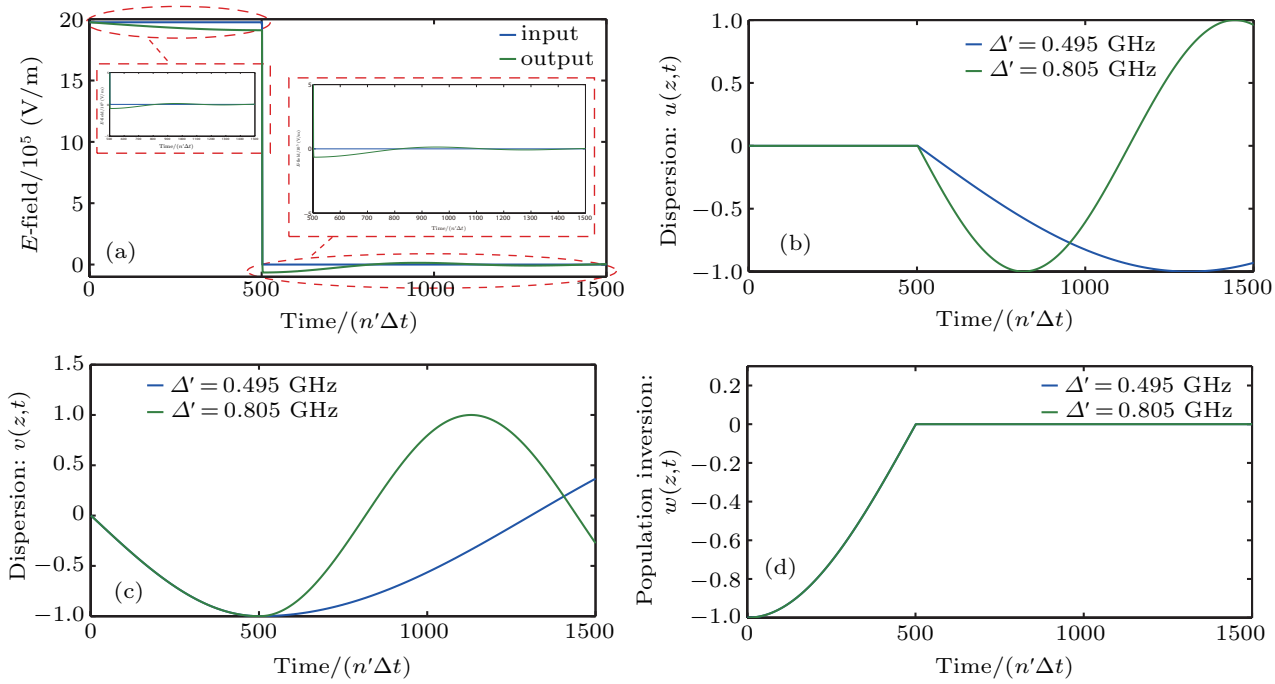



**Fig. 2.** (color online) Simulation results of the interaction between one pulse and crystal with the duration of the input pulse equal to $500n'\Delta t$ and the total simulation time being $1500n'\Delta t$. (a) Blue line: input pulse; green line: output pulse. Inset: the zoomed version of case (a); (b) dispersion: $u(z,t)$. Blue line: $\Delta' = 0.495$ GHz; Green line: $\Delta' = 0.805$ GHz. (c) absorption: $v(z,t)$. Blue line: $\Delta' = 0.495$ GHz; Green line: $\Delta' = 0.805$ GHz. (d) population inversion: $w(z,t)$. Blue line: $\Delta' = 0.495$ GHz; Green line: $\Delta' = 0.805$ GHz.

Since the duration of the input pulse is far less than $T_2$ and $T_1$, the influence of $T_2$ and $T_1$ can be ignored. The effect of the $\pi/2$ pulse on Bloch vectors are shown in Figs. 2(b)–2(d). When $0 < t < 500n\Delta t$, the pulse is applied which causes a 50% excitation and the population inversion $w(z,t)$ turn to 0 from $-1$. Since $\Delta = 0$, $\dot{u}(z,t)$ is equal to 0 and the dispersion $u(z,t)$ keeps unchanged. Accordingly, the absorption $v(z,t)$ changes into $-1$ from 0. The variation of $v(z,t)$ will results in the decreasing of pulse's field as is seen in the Fig. 2(a). Comparing with the previous results {Fig. 2(b) of Ref. [8]}, the simulation results in Fig. 2(a) are more in line with the actual situation for the field suffering decreasing instead of increasing at the beginning in absorbing medium.

When $t > 500n\Delta t$, the input pulse has been removed. Since $t_{\text{decay}} \ll T_1$, the value of population inversion $w(z,t)$ will keep unchanged and the Bloch vectors will rotate around $w$ axis in this process. Comparing the blue line and green line in Figs. 2(b) and 2(c), we can find that the rotate speed for Bloch vectors with different $\Delta'$ exists differences. The rotation speed is faster when $\Delta'$ is larger. This means that the Bloch vector will not keep in phase which leads to the decreasing of the induced field.

This section presents more details of the interaction between one pulse and the crystal by FDTD method. This method can also be used to display the generation of 3PE which is derived from the interaction between three pulses with the crystal. The performances are shown in the following part.

## 3. Simulation of 3PE

In this part the formation process of 3PE is presented in which the influence of pulses' area is discussed. Then, the impact of thickness is analyzed.

The parameters of the simulation for 3PE are from

Ref. [8]. The first pulse is applied at $t = 0$ and removed at$t = t_1' = 500n'\Delta t$; The second pulse is shot into crystal at $t = t_2 = 1500n'\Delta t$ and removed at $t = t_2' = 2000n'\Delta t$; The last pulse is shot into crystal at $t = t_3 = 5000n'\Delta t$ and removed at $t = t_3' = 5500n'\Delta t$. The amplitude of each pulse is $1.9738 \times 10^6$ V/m which makes sure that $\theta_1 = \theta_2 = \theta_3 = \pi/2$. The basic parameters of crystal keep unchanged. Namely, the $\alpha'$ is also equal to 280.

Figure 3 shows the simulation results of 3PE with $L = 0.01$ cm.

Figure 3(a) shows that the peak value of 3PE appears at $t_{3\mathrm{PE}}$ after the interaction between three pulses and crystal, where $t_{3\mathrm{PE}} = t_3' + (t_2 - t_1')$. Figures 3(b)–3(d) show the effect of input pulses on Bloch vectors. The first pulse stimulates the atoms to excited state and population inversion $w(z,t)$ changes from $-1$ to 0. The absorption $v(z,t)$ becomes $-1$ at $t = 500n\Delta t$. When $t_1' < t < t_2$, the first pulse is removed. The dispersion $u(z,t)$ will not keep 0 any more and the Bloch vectors rotate around $w$ axis and away from $v$ axis. When $t_2 < t < t_2'$ , the second pulse is shot into the crystal and more atoms are stimulated into excited state. Accordingly, the value of population inversion $w(z,t)$ will change into a positive value. Then, the second pulse is removed, the Bloch rotates around $w$ axis again. By applying the third pulse at $t = t_3$, the atoms on the excited state will transit to ground state and the population inversion $w(z,t)$ changes into 0. When $t_3' < t$, the Bloch vectors will rotate close to $v$ axis and the absorption $v(z,t)$ achieves the maximum at $t_{3\mathrm{PE}} = 6500n'\Delta t$.

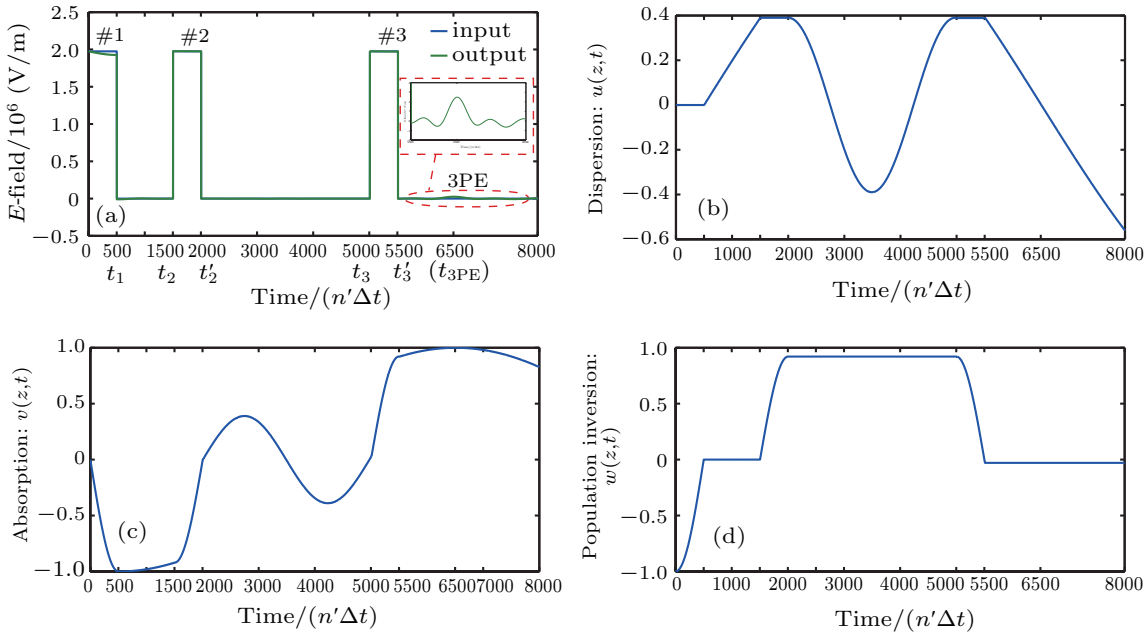



**Fig. 3.** (color online) (a) simulation results of 3PE with $L = 0.01$ cm. Blue line: input; Green line: output. Inset: the zoomed version of 3PE field. (b)–(d) The variations of $[u(z,t), v(z,t), w(z,t)]$ over time, with $\Delta'$ set as 0.04 GHz for $t_1' < t < t_2$ and 0.846 GHz for $t_2' < t < t_3$, which just achieves $[0,1,0]$ at $t = t_{3\mathrm{PE}}$.

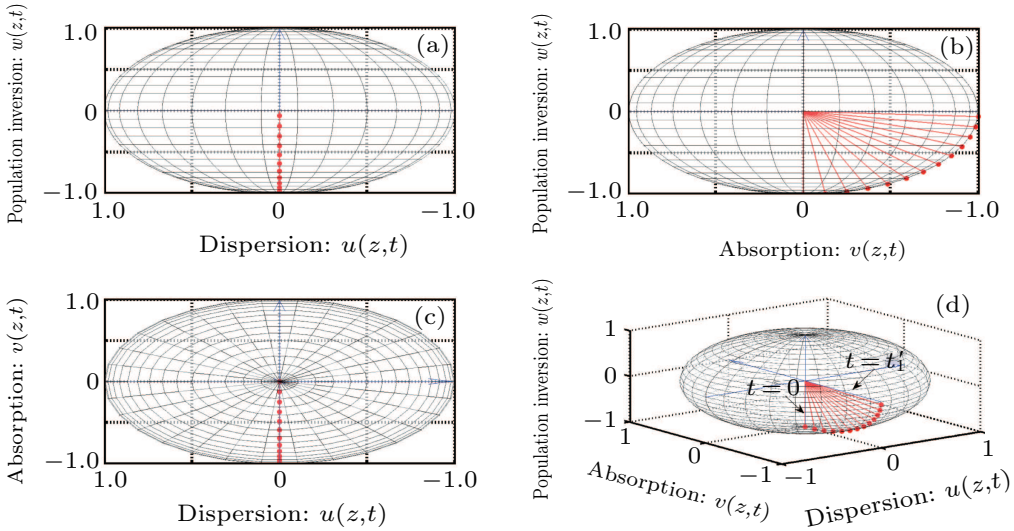



**Fig. 4.** (color online) Rotation of Bloch vectors with the first pulse applied: (a) $u$–$w$ plane, (b) $v$–$w$ plane, (c) $u$–$v$ plane, (d) three-dimensional diagram.

### 3.1. The formation process of 3PE

In order to present the generation of 3PE vividly and explain why $t_{3\mathrm{PE}} = t_3' + t_2 - t_1'$, we explore the rotation of Bloch vectors over time in three-dimensional Bloch sphere with $\Delta'$ set as $\pm 0.04$ GHz for $t_1' < t < t_2$ and $\pm 0.846$ GHz for $t_2' < t < t_3$.

Figure 4 shows the rotation of Bloch vectors when the first pulse is applied.

When $0 < t < t_1'$, the dispersion $u(z,t)$ keeps unchanged and the Bloch vectors rotate around $u$ axis. The rotation angle is equal to $\theta_1 = \pi/2$ and Bloch vectors will rotate from $[0,0,-1]$ to $[0,-1,0]$ as shown in Fig. 4(d).

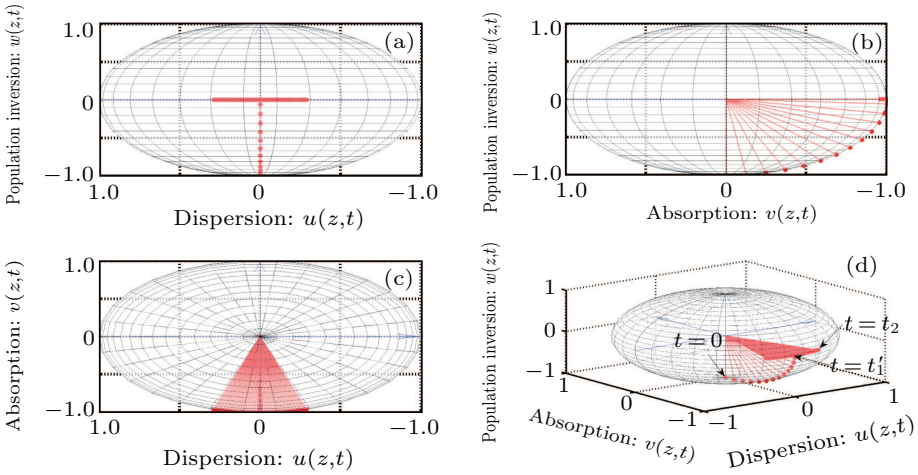



**Fig. 5.** (color online) Rotation of Bloch vectors with first pulse removed: (a) $u$–$w$ plane, (b) $v$–$w$ plane, (c) $u$–$v$ plane, (d) three-dimensional diagram.

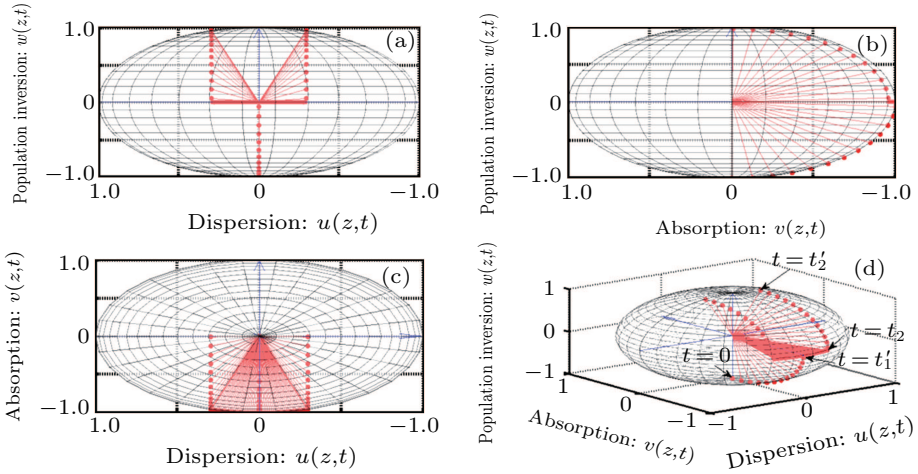



**Fig. 6.** (color online) Rotation of Bloch vectors with the second pulse shot into crystal: (a) $u$–$w$ plane, (b) $v$–$w$ plane, (c) $u$–$v$ plane, (d) three-dimensional diagram.

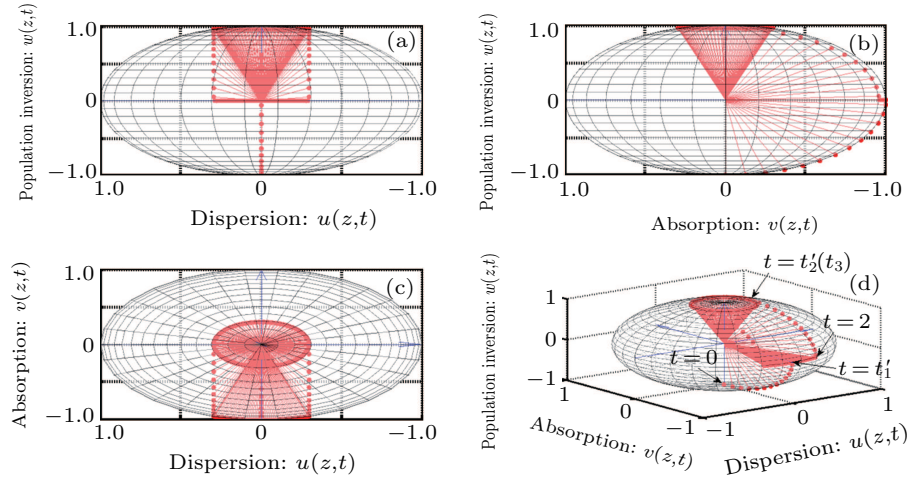



**Fig. 7.** (color online) Rotation of Bloch vectors with the second pulse passing through the crystal: (a) $u$–$w$ plane, (b) $v$–$w$ plane, (c) $u$–$v$ plane, (d) three-dimensional diagram.

When $t_1' < t < t_2$, the first pulse is removed. The rotation of the Bloch vectors in this process is shown in Fig. 5.

In this process, the Bloch vectors rotate around $w$ axis and the rotation angle is equal to $|\Delta'| \cdot (t_2 - t_1')$. Here, $\Delta'$ is set as $\pm 0.04$ GHz. For $\Delta' > 0$, the Bloch vector will rotate anticlockwise. Oppositely, the Bloch vector will rotate clockwise with $\Delta' < 0$. This means that the dipole moments are in the de-phasing process.

When $t_2 < t < t_2'$, the second pulse is shot into crystal.

In this process, the Bloch vectors rotate around $u$ axis. The Bloch vector will stop on $u$–$w$ plane at $t = t_2'$ since $\theta_2$ is equal to $\pi/2$.

After the second pulse passing through the crystal, the rotation of Bloch vectors in this process is depicted in Fig. 7.

The same as Fig. 5, the Bloch vectors will rotate along the opposite direction on a certain plane when the second pulse is removed.

Figure 8 presents the rotation of Bloch vectors when the third $\pi/2$ pulse is applied.

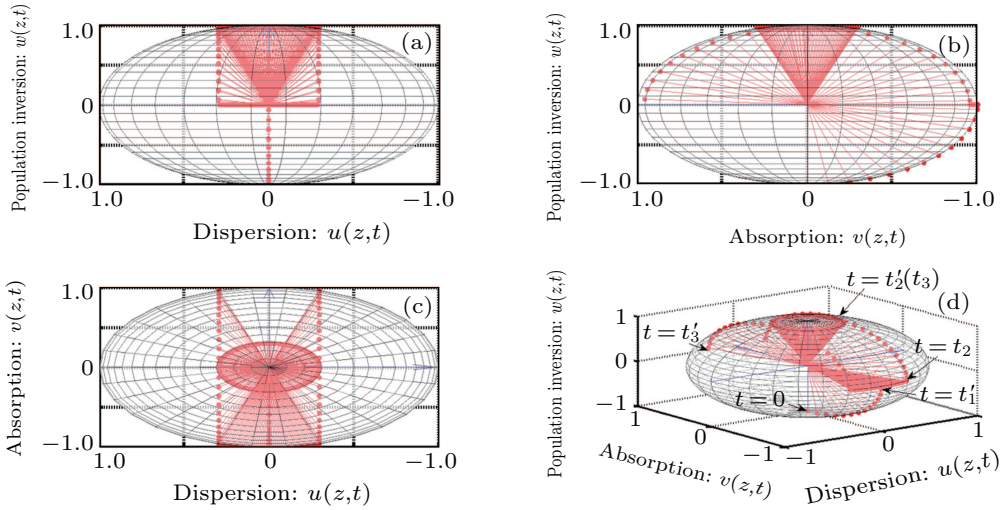



**Fig. 8.** (color online) Rotation of Bloch vector with the third $\pi/2$ pulse applied: (a) $u$–$w$ plane, (b) $v$–$w$ plane, (c) $u$–$v$ plane, (d) three-dimensional diagram.

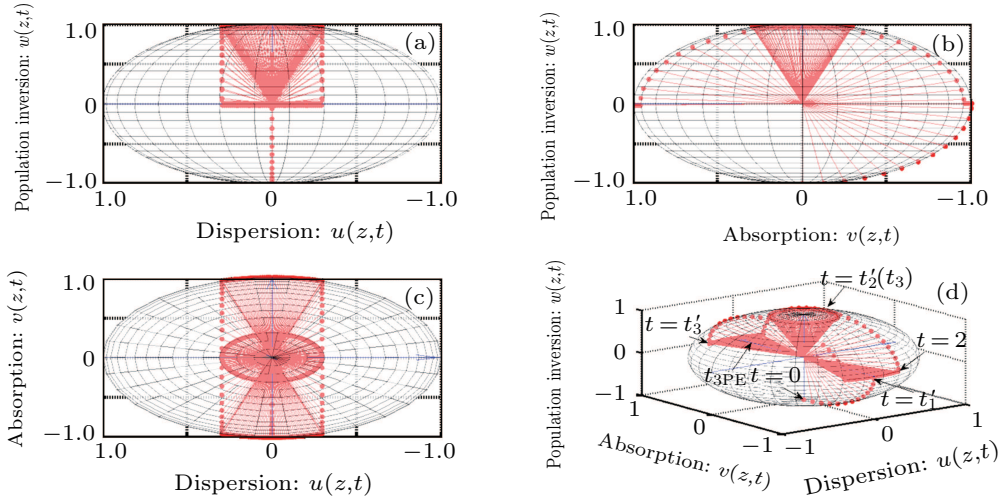



**Fig. 9.** (color online) Rotation of Bloch vectors with the third pulse removed: (a) $u$–$w$ plane, (b) $v$–$w$ plane, (c) $u$–$v$ plane, (d) three-dimensional diagram.

The Bloch vectors rotate around $u$ axis with the rotation angle equal to $\pi/2$ and the Bloch vectors will stop on $u$–$v$ plane at $t = t_3'$.

When $t_3' < t$, the Bloch vectors rotate around $w$ axis and will spend the time ,which is equal to the interval between first pulse and second pulse $(t_2 - t_1')$, incorporating two different frequency shift components of atoms on the $u$–$v$ plane and achieving $[0,1,0]$ when $t = t_3' + (t_2 - t_1')$. This represents that dipole moments reach their maximum and phases of different dipole moments tend to be accordance which results in the generation of 3PE. The process is shown in Fig. 9.

### 3.2. Influence of input pulses' area on 3PE's amplitude

According to Eq. (7), the amplitude of 3PE is associated with the value of absorption $v(z,t)$ at $t = t_{3\mathrm{PE}}$ which are affected by the rotation angle of Bloch vectors. As is shown in Figs. 4–9, when the incident pulse is applied, the rotation angle of Bloch vectors is equal to the area of the pulse. That is,

the variation of input pulses' area will influence the amplitude of 3PE field. Figure 10 shows the relationship between the amplitude of 3PE and the sum of three-pulse's area.

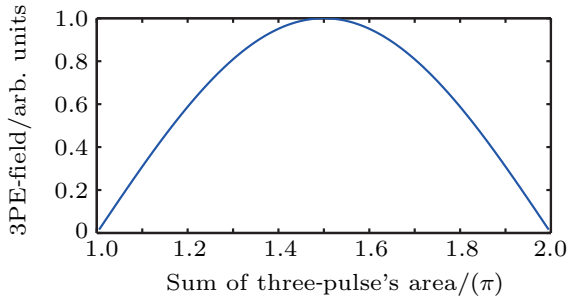



**Fig. 10.** (color online) 3PE-field versus the sum of three-pulse's area curve.

As is shown in Fig. 10, the 3PE's amplitude will achieve maximum when the sum of three-pulse's area is equal to $3\pi/2$. This is because the Bloch vectors will fail to stop on $u$–$v$ plane and achieve $[0,1,0]$ at $t_{3\mathrm{PE}}$ when the sum of the three-pulse's area is not $3\pi/2$.

### 3.3. Influence of thickness on 3PE's amplitude

In Refs. [10] and [11], the influence of thickness had not been discussed for the thickness smaller than the actual situation in their simulation. However, this influence cannot be ignored in thick crystal.

Figure 11 shows the output of 3PE with $L = 0.01$ cm, $L = 0.1$ cm, and $L = 0.2$ cm.

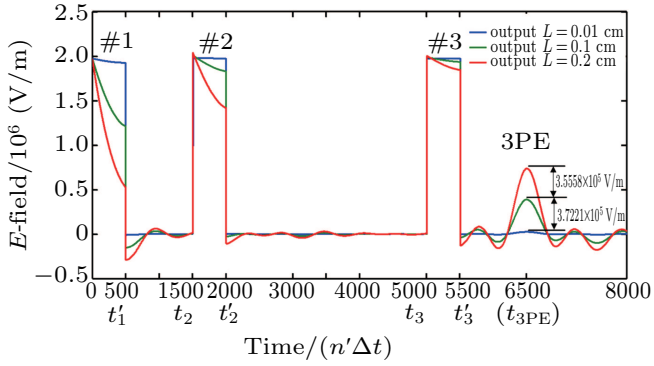



**Fig. 11.** (color online) Sequences of output for 3PE with $L = 0.01$ cm, $L = 0.1$ cm, and $L = 0.2$ cm.

As is shown in Fig. 11, the 3PE field will be improved when the thickness increases. Meanwhile, we find that the increment of 3PE field is $3.7221 \times 10^5$ V/m when the thickness ranges from 0.01 cm to 0.1 cm and turns to $3.5558 \times 10^5$ V/m when the thickness ranges from 0.1 cm to 0.2 cm. This means that the increment of 3PE field will decrease with the increasing of thickness. This phenomenon can also explained by Bloch vector.

According to Eq. (7), the increment of 3PE field is connected with the absorption $v(z,t)$ at $t = t_{3\mathrm{PE}}$. With the numerical solution, we illustrate the value of $v(z,t_{3\mathrm{PE}})$ for the thickness ranging from 0 cm to 0.75 cm in Fig. 12.

During the propagation, the amplitude of input pulse will be attenuated and the sum of three-pulse's area would not keep $3\pi/2$ which results in the Bloch vector failing to arrive on $u$–$v$ plane and reach $[0,1,0]$ at $t_{3\mathrm{PE}}$. From the plots of Fig. 12, it can be seen that the value of $v(z,t_{3\mathrm{PE}})$ at each position is not same and decreases from 1 to 0 gradually with the increasing of thickness.

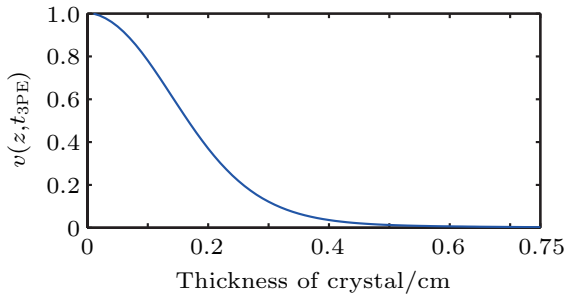



**Fig. 12.** (color online) The value of $v(z,t_{3\mathrm{PE}})$ for the thickness ranging from 0 cm to 0.75 cm.

Combing the simulation results in Fig. 12 and Eq. (7), we present the trend of the 3PE field with the increasing of thickness in Fig. 13.

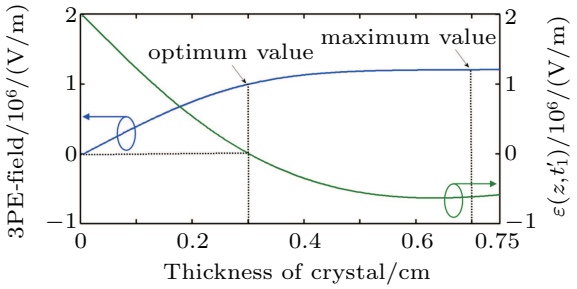



**Fig. 13.** (color online) Blue line: trend of the 3PE-field with the increasing of thickness. Green line: the variation of first pulse's amplitude $\varepsilon_{n1}(z,t)$ at $t = t_1'$.

The blue line in Fig. 13 shows that the maximum amplitude of 3PE field is attained when the thickness is 0.7 cm. In practice, the numerical maximum may not be the optimum value when the attenuation of input pulse is considered. If the input pulse field becomes negative, the result of the iteration is meaningless. Thus, it is necessary to not only find the thickness that get the maximum echo amplitude, but which also make sure that the input pulse is positive duration the propagation process. The green line shows that the value of $\varepsilon_{n1}(z,t_1')$ has been decreased to 0 when the thickness is 0.3 cm, where $\varepsilon_{n1}(z,t_1')$ is the amplitude of first pulse field at $t_1'$. According to the simulation results in Fig. 13, we can get the conclusion that the optimum thickness to generate 3PE is 0.3 cm for $Tm^{3+}$:YAG whose linear resonant absorption coefficient $\alpha'$ is equal to 280.

### 3.4. Influence of thickness on 3PE's efficiency

The variations of the input pulse and the 3PE over the propagation direction will lead to the variation of 3PE's efficiency which is expressed as[8]

$$\eta_{\mathrm{echo}}(\alpha' z) = |\varepsilon_{3\mathrm{PE}}(z,t)|_{t=t_{3\mathrm{PE}}}|^2 / |\varepsilon_{n1}(z,t)|_{t=t_1'}|^2. \quad (8)$$

With the numerical solutions of first pulse and 3PE achieved, the curve of the efficiency with the increasing of thickness is presented in Fig. 14.

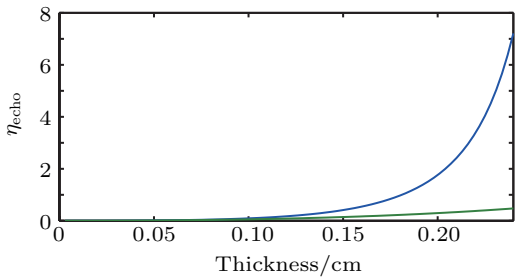



**Fig. 14.** (color online) The curve of the efficiency with the increasing of thickness. Green line: the simulation result conducted based on the Eq. (20) of Ref. [8]. Blue line: the simulation result conducted based on Eq. (7) and Eq. (8) in this paper.

The efficiency of 3PE in Ref. [8] is conducted with $|\varepsilon_{3\rm PE}(t)|_{t=t_{3\rm PE}}|^2/(|\varepsilon_{n1}(0,t)|_{t=t_1'}|^2\,{\rm e}^{-\alpha' L})$. The flaws of this expression are that the propagation of 3PE is not taken into consideration and $|\varepsilon_{n1}(z,t)|_{t=t_1'}|^2 = |\varepsilon_{n1}(0,t)|_{t=t_1'}|^2\,{\rm e}^{-\alpha' L}$ is only appropriate for the pulse's area being very small. The green line in Fig. 14 shows the corresponding simulation result which is expressed as $0.09\exp(\alpha' L)$. The Blue line shows the result which is conducted with Eq. (7) and Eq. (8) in this paper. By contrast, we find the expression to describe the relationship between efficiency and thickness should be modified as $1.3\cdot 0.09\exp(2.4\cdot\alpha' L)$. The root-mean-square error of modified expression is 0.06637.

## 4. Conclusion

In this paper, the phenomenon of 3PE in thick crystal is investigated with M-B equations solved by FDTD method. Firstly, the formation process of 3PE is presented based on the rotation of the Bloch vectors. We verify that the interval between 3PE and third pulse equals to the interval between the first two pulses. Meanwhile, we demonstrate the 3PE's amplitude will achieve maximum when the sum of the three-pulse's area is $3\pi/2$. Then, the influence of thickness on 3PE's amplitude and efficiency is investigated. We find that the 3PE's amplitude will increase with the increasing of thickness and the optimum thickness is 0.3 cm for $Tm^{3+}$:YAG when the attenuation of the input pulse is taken into consideration. According to the simulation results, we also find the expression which describes relationship of echo's efficiency and optical thickness should be modified as $1.3\cdot 0.09\,{\rm e}^{2.4\cdot\alpha' L}$.

## References

[1] Bonarota M, Ruggiero J, Gouët J L L and Chaneliére T 2010 *Phys. Rev. A* **81** 76
[2] Chaneliére T, Ruggiero J, Bonarota M, Afzelius M and Gouët J L L 2009 *New J. Phys.* **12** 802
[3] Damon V, Crozatier V, Chaneliére T, Jean-Louis Le Gouet and Ivan Lorgere 2010 *J. Opt. Soc. Am. B* **27** 524
[4] Barber Z, Tian M, Reibel Rand Babbitt W R 2002 *Opt. Express* **10** 1145
[5] Ma X R, Wang S, Zhang S G, Zhang S Y and Liang Y Q 2015 *IEEE Commun. Lett.* **19** 179
[6] Ma X R, Wang S, Liang Y Q and Shan Y L 2015 *Appl. Opt.* **54** 2891
[7] Sangouard N, Simon C 2010 *Phys. Rev. A* **81** 062333
[8] Ma X R, Liang Y Q, Wang S, Zhang S G and Shan Y L 2016 *Chin. Phys. B* **25** 070302
[9] Ziolkowski R W, Arnold J M and Gogny D M 1995 *Phys. Rev. A* **52** 3082
[10] Schlottau F, Piket-May M and Wagner K 2005 *Opt. Express* **13** 182
[11] Tiranov A D, Karimullin K R and Samartsev V V 2012 *Bull. Russ. Acad. Sci. Phys.* **76** 299
[12] Ma X R, Zhang S Y and Zhang S G 2014 *Chin. Phys. B* **23** 060304
[13] Brewer R G and Shoemaker R L 1971 *Phys. Rev. Lett.* **27** 631
[14] Pierre Meystre and Murray Sargent III 2007 *Elements of Quantum Optics*, 4th edn. (Springer Press) pp. 6–7
[15] McCall S L and Hahn E L 1969 *Phys. Rev.* **183** 457
[16] Alekseyev A I and Basharov A M 1981 *Opt. Commun.* **36** 291
[17] Endo T, Nakanishi S, Muramoto T and Hashi T 1981 *Opt. Commun.* **37** 369